J. Am. Chem. Soc.

Charge Carrier Formation in Polythiophene/Fullerene Blend Films Studied by Transient Absorption Spectroscopy

Hideo Ohkita,[*,†,#] Steffan Cook,[†] Yeni Astuti,[†] Warren Duffy,[‡] Steve Tierney,[‡] Weimin Zhang,[‡] Martin Heeney,[‡,||] Iain McCulloch,[‡,⊥] Jenny Nelson,[§] Donal D. C. Bradley,[§] and James R. Durrant[*,†]

Department of Chemistry, Imperial College London, Exhibition Road, London SW7 2AZ, United Kingdom, Merck Chemicals, Chilworth Science Park, Southampton SO16 7QD, United Kingdom, and Department of Physics, Imperial College London, Prince Consort Road, London SW7 2BW, United Kingdom

E-mail: ohkita@photo.polym.kyoto-u.ac.jp; j.durrant@imperial.ac.uk

Abstract: We report herein a comparison of the photophysics of a series of polythiophenes with ionization potentials ranging from 4.8 to 5.6 eV as pristine films and when blended with 5 wt% 1-(3-methoxycarbonyl)propyl-1-phenyl-[6,6]C_{61} (PCBM). Three polymers are observed to give amorphous films, attributed to a non-planar geometry of their backbone whilst the other five polymers, including poly(3-hexylthiophene), give more crystalline films. Optical excitation of the pristine films of the amorphous polymers is observed by transient absorption spectroscopy to give rise to polymer triplet formation. For the more crystalline pristine polymers, no triplet formation is observed, but rather a short-lived (~ 100 ns), broad photoinduced absorption feature assigned to polymer polarons. For all polymers, the addition of 5 wt% PCBM resulted in 70 – 90% quenching of polymer photoluminescence (PL), indicative of efficient quenching of polythiophene excitons. Remarkably, despite this efficient exciton quenching, the yield of dissociated polymer$^+$ and PCBM$^-$ polarons, assayed by the appearance of a long-lived, power-law decay phase assigned to bimolecular recombination of these polarons, was observed to vary by over two orders of magnitude depending upon the polymer employed. In addition to this power-law decay phase, the blend films exhibited short-lived decays assigned, for the amorphous polymers, to neutral triplet states generated by geminate recombination of bound radical pairs and, for the more crystalline polymers, to the direct observation of the geminate recombination of these bound radical pairs to ground. These observations are discussed in terms of a two-step kinetic model for charge generation in polythiophene/PCBM blend films analogous to that reported to explain the observation of exciplex-like emission in poly(*p*-phenylenevinylene)-based blend films. Remarkably, we find a excellent correlation between the free energy difference for charge separation (ΔG_{CS}^{rel}) and yield of the long-lived charge generation yield, with efficient charge generation requiring a much larger ΔG_{CS}^{rel} than that required to achieve efficient PL

quenching. We suggest this observation is consistent with a model where the excess thermal energy of the initially formed polarons pairs is necessary to overcome their coulomb binding energy. This observation has important implications for synthetic strategies to optimize organic solar cell performance, as it implies that, at least devices based on polythiophene/PCBM blend films, a large ΔG_{CS}^{rel} (or LUMO level offset) is required to achieve efficient charge dissociation.

Introduction

Great progress has now been made in our understanding of photoinduced electron transfer in isolated donor–acceptor (D–A) molecular systems.[1–5] Inspired by the remarkable photophysics and photochemistry of photosynthetic reactions centers, increasingly sophisticated D–A molecular relays have been synthesized and characterized in solution.[6,7] Such molecular relays have been designed for the directional electron transfer driven by appropriate energetic cascades, resulting in sequential charge separations and generating a long-lived, spatially separated charge separated states or 'radical pairs'.[8–10]

On the other hand, reports of efficient photoinduced charge separation in solid state blend films of conjugated polymers with fullerenes[11,12] have attracted increasing interest due to their applicability to photovoltaic (PV) solar energy conversion. The intermixing of the polymer electron donor with the fullerene electron acceptor in such blended films (the formation of a 'bulk heterojunction') can result in a significant enhancement of photoinduced charge separation in such films relative to more conventional bilayered heterojunction devices.[13] Currently, power conversion efficiencies approaching 5% have been reported by several groups for organic PV devices based on blend films of regioregular poly(3-hexylthiophene) (P3HT) and 1-(3-methoxycarbonyl)propyl-1-phenyl-[6,6]C_{61} (PCBM).[14–19] Most studies of such blend films have focused on the optimization of PV device performance through control of materials structure, film processing conditions, and blend morphology. Device performance has been shown to be significantly affected by thermal treatments,[19,20] blend composition,[21,22] solvents,[23] film thickness,[24] regioregularity of conjugated polymers,[17] and molecular weight.[25] Recent systematic studies with various conjugated polymers and fullerenes have demonstrated that open-circuit voltage V_{OC} is directly correlated with the HOMO level of the conjugated polymer[26] and

the LUMO levels of fullerene.[27] However systematic studies of the photophysics and photochemistry of polythiophene/PCBM blend films as a function of polymer properties, and their correlation with device performance, have received limited attention to date. Most typically photoluminescence (PL) emission quenching is employed to assay the quenching of photogenerated polythiophene excitons by PCBM, with efficient emission quenching being regarded as an indicator of efficient charge photogeneration. In this paper we report a detailed study of the photophysics and photochemistry of polythiophene/PCBM blend films employing eight different thiophene-based polymers. In all cases, efficient quenching of the polymer PL is observed by the inclusion of only 5 wt% PCBM, indicative of efficient quenching of the polymer excitons. Transient absorption spectroscopy is employed to determine the photogenerated species resulting from this exciton quenching. Remarkably, despite the similar emission quenching observed for all polymers studied, the yield of long-lived photogenerated charges is found to vary by two orders of magnitude depending upon polymer employed.

Studies of the photophysics and photochemistry of organic blend films to date have largely focused on polymer/fullerene and polymer/polymer blend films employing poly(*p*-phenylenevinylene) (PPV) based polymers.[28–30] Such blend films have been shown to give PV devices, although with more modest solar energy conversion efficiencies than polythiophene-based devices. In PPV-based polymer/polymer blend films, charge photogeneration has been described as a two-step process. Initial charge separation at the donor/acceptor interface has been suggested to result in the formation of a coulombically bound radical pair (BRP) state. Such BRPs are analogous to the 'contact ion pairs' discussed in solution studies of molecular D–A systems.[9,10] For the PPV-based polymer/polymer blends, this BRP state has been shown to exhibit a red-shifted emission band,[29–32] analogous to the emission of donor/acceptor excited state

complexes or 'exciplexes'.[33,34] This BRP state can undergo rapid intersystem crossing between its singlet and triplet states. Dissociation of this BRP to free charges competes with its geminate recombination either to the singlet ground state S_0 or to neutral triplet excitons, depending upon the radical pair spin state. This geminate recombination, which should be distinguished from the subsequent bimolecular recombination of the dissociated free charges, has been suggested to be a key factor in limiting device performance for PPV-based devices. Similar observations have been made for polyfluorene-based polymer/polymer blend films[35] and for polyfluorene/fullerene blends.[36] In particular, in a study employing three different PPV-based polymers, an inverse correlation was observed between this exciplex-like emission strength and PV device performance.[32] However, a clear understanding of the parameters determining the efficiency of charge dissociation versus geminate recombination in organic blend films is yet to be established. Moreover such studies have not previously focused on polythiophene materials, the polymer class currently attracting the greatest interest for efficient organic PV cells.

We have previously reported photophysical studies of polythiophene/fullerene blend films, employing transient absorption spectroscopy with low intensity excitation pulses. For P3HT/PCBM blend films, a high yield of photogenerated charge carriers is observed. These charge carriers exhibit dispersive, bimolecular recombination characterized by a power-law decay.[17] We have recently extended these studies to two higher ionization potential (IP) thiophene-based copolymers.[37] In contrast to P3HT, quenching of the polymer singlet exciton by the inclusion of PCBM was shown to generate a high yield of triplet excitons rather than dissociated polarons. This was attributed to efficient triplet formation through geminate charge recombination of bound triplet radical ion pairs,[37] analogous to that also reported for polymer/polymer blend films.[35,38] Our observation of triplet formation rather than polaron

formation for two higher IP polythiophenes indicates that polymer IP may play a role in influencing the blend photophysics. This result parallels our recent investigation of a polyfluorene/PCBM blend film where we concluded that the high IP of the polyfluorene prevented photoinduced charge separation but rather resulted in Förster energy transfer to the PCBM and subsequent intersystem crossing from the PCBM singlet to triplet exciton.[39] Analogous energy transfer dynamics have also been observed for dye-doped conjugated polymer films.[40] These findings have motivated us to undertake a more in-depth study of the photophysical processes in polythiophene/PCBM blend films as a function of polythiophene IP. To control the polymer IP, we have chemically modified the backbone structure to achieve a perturbation of the π electron conjugation. Sterically forcing a twist between neighboring units has been shown to reduce the π orbital overlap in the conjugation backbone, thereby raising the polymer IP.[41,42] Alternatively introducing a non- or less-conjugated unit as a component of the polymer backbone has also been shown to increase the polymer IP.[43–45] On the basis of these strategies, we have prepared a series of polythiophenes with IPs ranging from 4.8 to 5.6 eV. Higher IP polythiophenes are particularly interesting because of their potential to increase cell V_{OC} relative to that achievable by P3HT.[26] These polythiophenes enable us to vary systematically the energetics of charge separation in blend films with the electron acceptor PCBM. Charge carriers and triplet excitons formed in a series of such blend films are directly observed by transient absorption spectroscopy, and analyzed in terms of a two-step model for charge generation. In all cases, our studies are limited to comparison of pristine polymer films with those with 5 wt% added PCBM. The low PCBM concentration was selected to avoid the morphological changes to the polythiophene widely reported to result from the addition of high PCBM concentrations.[21] For all polymers, this low concentration of PCBM was sufficient to

result in efficient (> 70%) emission quenching, indicative of efficient polymer exciton quenching. We note that caution should be taken in relating measurements taken at this PCBM concentration directly to PV device performance which is typically measured at higher (> 50 wt%) PCBM concentrations, and emphasize that the primary motivation of these studies is a fundamental understanding of the photophysics of polythiophene/PCBM interfaces rather than a direct correlation with device performance.

Experimental Section

Materials. Seven kinds of novel polythiophenes were synthesized as reported elsewhere.[41–43] 1-(3-Methoxycarbonyl)propyl-1-phenyl-[6,6]C_{61} (PCBM) was kindly supplied from the University of Groningen and used as received.[46] To the polythiophene and PCBM added chlorobenzene (Aldrich) at a concentration of ~ 10 mg mL^{-1}. For P($T_{12}T_{12}TT_0$), P($T_0T_0TT_{16}$), P(T_0TT_{16}), and P($T_{12}SeT_{12}$), the solution was heated in a water bath at 100 °C for a few minutes to be dissolved homogeneously. Polymer films were spin-coated onto glass substrates at a spin rate of 3000 rpm for 90 s from the chlorobenzene solution under nitrogen atmosphere. The weight concentration of PCBM in the final polymer blend films was fixed at 5 wt%. Before the spin-coating, the substrates were pre-cleaned by sonication in toluene, acetone, and ethanol for 15 min, respectively. For *J*–*V* characteristics measurements, PV devices were fabricated as reported previously.[17]

Measurements. Molecular weight determinations were carried out in chlorobenzene solution on an Agilent 1100 series HPLC using two Polymer Laboratories mixed B columns in series, and the system was calibrated against narrow weight polystyrene calibration standards (Polymer Laboratories). Hole mobility was evaluated from the linear fit of the root square of

the source–drain current in the saturated regime versus the gate voltage by the field-effect transistor (FET) measurements as described elsewhere.[41,44] Ionization potential (IP) of the polymer pristine films was measured by an ambient ultraviolet photoelectron spectroscopy (UPS) technique with a UPS spectrometer (Riken-Keiki, AC-2). X-ray diffraction (XRD) measurements were carried out with an X-ray diffractometer (Philips, PW1710). Absorption and PL spectra were measured at room temperature with a UV–visible spectrophotometer (Shimadzu, UV-1601) and a spectrofluorimeter (Horiba Jobin Yvon, Spex Fluoromax 1), respectively. The energy-minimized molecular structures of oligothiophene units were calculated using MOPAC program (CambridgeSoft). Transient absorption data were collected with a highly sensitive microsecond transient absorption system under Ar or O_2 atmosphere as described elsewhere.[47] The excitation wavelength was 420 nm for P(T_{10}PhT_{10}), P(T_{12}NpT_{12}), and P($T_8T_8T_0$) and 530 nm for P3HT, P($T_{12}T_{12}TT_0$), P($T_0T_0TT_{16}$), P(T_0TT_{16}), and P(T_{12}SeT_{12}) unless otherwise noted. Low intensity excitation conditions (5 – 65 μJ cm^{-2}) were employed to ensure that the densities of photogenerated charge carriers are comparable to those generated under solar irradiation (10^{17} – 10^{18} cm^{-3}). *J–V* characteristics of blend films were measured under 50 mW cm^{-2} simulated sunlight (AM1.5) under N_2 atmosphere.

Results

Characterization of Polythiophene Pristine Films. Table 1 summarizes the molecular weights, hole mobilities, and IPs of the polymers employed in this study. The polymers exhibited weight average molecular weights (M_w) in the range 20,000 – 100,000, with a polydispersity index (M_w/M_n) of approximately 2. In terms of their materials properties, these

polymers can be effectively divided into two distinct groups. $P(T_{10}PhT_{10})$, $P(T_{12}NpT_{12})$, and $P(T_8T_8T_0)$ were easily soluble in chlorobenzene at room temperature and formed uniform and smooth films by spin-coating from the chlorobenzene solution. Differential scanning calorimetry (DSC) data of the bulk powders indicates that $P(T_8T_8T_0)$ is amorphous, whilst $P(T_{10}PhT_{10})$ and $P(T_{12}NpT_{12})$ do show melting and recrystallization behavior but with rather low recrystallization enthalpies (8 and 5 J g^{-1} respectively).[41] However XRD data indicated that thin films prepared by spin-coating were amorphous (see supporting information). In contrast, $P(T_{12}T_{12}TT_0)$, $P(T_0T_0TT_{16})$, $P(T_0TT_{16})$, and $P(T_{12}SeT_{12})$ were hardly soluble in chlorobenzene at room temperature, but soluble at 100 °C and formed less uniform films. XRD indicated that these films are significantly more crystalline (see supporting information) and showed similar peaks to P3HT. As summarized in Table 1, the amorphous polymers exhibited relatively large IPs and lower carrier mobilities, on the order of 10^{-5} to 10^{-4} cm^2 V^{-1} s^{-1} as determined by FET measurements. We note that, due to these relatively low hole mobilities, the amorphous materials are not expected to make efficient PV devices. The more crystalline polymers exhibit higher carrier mobilities on the order of 10^{-1} cm^2 V^{-1} s^{-1} and relatively low IPs. It is worth noting that four of the crystalline polymers in this study exhibit higher hole mobilities than P3HT.

-----<<< Table 1 >>>-----

The photophysical properties of the pristine polymer films are summarized in Table 2. Figure 1 shows absorption and PL spectra of three representative polymer pristine films; $P(T_{10}PhT_{10})$ as an amorphous polymer, $P(T_0T_0TT_{16})$ as a partially crystalline polymer, and P3HT as a reference. The amorphous $P(T_{10}PhT_{10})$, $P(T_{12}NpT_{12})$, and $P(T_8T_8T_0)$ pristine films

exhibited structureless absorption bands at 416, 423, and 438 nm, respectively, which are significantly blue-shifted compared with the lowest vibrational band of P3HT (~ 640 nm). On the other hand, the more crystalline P($T_{12}T_{12}TT_0$), P($T_0T_0TT_{16}$), P(T_0TT_{16}), and P($T_{12}SeT_{12}$) pristine films exhibited more structured, red-shifted absorption bands with a shoulder or a vibrational band corresponding to the lowest vibronic transition at ~ 635, 612, 633, and ~ 640 nm, respectively, which is more comparable to that of P3HT (~ 640 nm). The vibrational structure observed is characteristic of ordered polythiophene films and is consistent with interplanar π-stacking of conjugated planes.[48] The corresponding PL spectra shows the same trends between the amorphous and more crystalline polymers, as summarized in Table 2. Note that the PL intensity of the amorphous polymers was generally much larger than that of the more crystalline polymers. From the absorption and PL spectra, the energy level of the lowest singlet excited state (S_1 or 'singlet exciton') E_S was evaluated to be 2.5 – 2.7 eV for the amorphous polymer pristine films, and ~ 2.0 eV for the more crystalline polymers. Furthermore, the Stokes shifts ΔE_{Stokes}, determined from the splitting of the absorption and emission bands, were also observed to be much larger for the amorphous polymer films compared with those of the more crystalline polymer films. This indicates a larger structural relaxation of the amorphous polymers following photoexcitation.[49]

-----<<< Figure 1 >>>-----

-----<<< Table 2 >>>-----

In order to address the origin of the different crystallinities observed for the two polymer

groups, we calculated molecular structures of oligomers as model compounds for P($T_{10}PhT_{10}$), P($T_0T_0TT_{16}$), and P3HT. The energy was minimized by MOPAC-AM2 calculations from an initial conformation optimized with the MM2 force-field. As shown in Figure 2, the P($T_{10}PhT_{10}$) oligomer exhibited a twisted structure in the backbone, attributed to the steric hindrance between a hydrogen atom of the phenyl (Ph) unit and the side chain of the 3-decylthiophene (T_{10}) unit, while the oligomers for P($T_0T_0TT_{16}$) and P3HT had a planar backbone. The Ph ring in the P($T_{10}PhT_{10}$) oligomer inclined at about 30° to the neighboring T_{10} units, suggesting localization of π-conjugation system. This twisted structure is consistent with the amorphous film morphology discussed above. In contrast, the dihedral angle of the neighboring two thiophene (T_0) units in the P($T_0T_0TT_{16}$) oligomer was almost 180° and that of the T_0 unit and a 3,6-dihexadecylthieno[3,2-*b*]thiophene (TT_{16}) unit was ~ 175°, suggesting more complete delocalization of the π-conjugation system along the more planar main chain, and consistent with the formation of more crystalline films. Furthermore, the dihedral angle of the neighboring two 3-hexylthiophene units in the P3HT oligomer was almost 180° indicating each 3-hexylthiophene unit is aligned in the same plane, consistent with previous reports.[17,50] These calculated dihedral angles are summarized in Table 3. We will discuss in detail later the distinct photophysical processes in pristine and blend films in terms of these molecular structures.

-----<<< Figure 2 >>>-----

-----<<< Table 3 >>>-----

Transient Absorption of Pristine Films. Transient absorption studies of the organic films were undertaken employing low intensity excitation conditions corresponding to approximately $10^{17} – 10^{18}$ absorbed photons cm^{-3}, comparable to the charge carrier densities generated in polymer/fullerene blend cells under solar irradiation. We consider first the results obtained for pristine, amorphous films, again using P($T_{10}PhT_{10}$) as the representative polymer. Pristine films of this polymer exhibited a photoinduced transient absorption band at around 700 nm, as shown in Figure 3. The transient signal decayed monoexponentially with a lifetime of 7 μs under Ar atmosphere, accelerating to ~ 1.5 μs under O_2 atmosphere. As already reported, the P($T_{10}NpT_{10}$) and P($T_8T_8T_0$) pristine films also exhibited similar O_2-sensitive transient photoinduced absorption bands around 800 nm with lifetimes of several microseconds.[37] These transient bands are assigned, as previously,[37] to a $T_1 \rightarrow T_n$ transitions of polymer triplet excitons ($^3P^*$) formed in the amorphous polymer pristine films. No distinct long-lived transients were observed for the pristine films.

-----<<< Figure 3 >>>-----

On the other hand, the P($T_0T_0TT_{16}$) pristine film, representative of the more crystalline polymers, exhibited a broader transient photoinduced absorption band around 900 – 1000 nm as shown in Figure 4. This transient optical density was much smaller than that observed for the amorphous polymers and decayed rapidly on the hundreds of nanoseconds timescale, down to less than 10^{-5} ΔOD within 1 μs. This decay is much faster than that of triplet excitons observed for the amorphous polymers. This fast transient was not quenched under O_2 atmosphere, as shown in the inset to Figure 4. These observations suggest that this absorption transient should

not be assigned to triplet excitons. On the other hand, it is too long lived to be assigned to singlet excitons; the luminescence lifetime is reported to be < 1 ns for regiorandom poly(3-octylthiophene) (P3OT) solution[51] and regioregular P3HT pristine film.[52] Indeed, no transient absorption ascribable to singlet excitons was observed for all the polymers studied herein on the timescales (> 200 ns). A similar absorption band has been reported for a regioregular P3HT pristine film by continuous wave photoinduced absorption (PIA) measurements at 10 K. The PIA spectrum exhibits an absorption peak around 990 nm (1.25 eV), and was assigned to localized polarons in the disordered portions of the film.[53] Similar rapid decays were observed for the other polythiophene pristine films. Thus, these rapid decays were ascribed to the charge recombination of polaron pairs formed in the pristine film. For the P3HT pristine film, no distinct transient signal was detected at room temperature within our time resolution, although a similar, broad, short-lived absorption transient was observed at 77 K.[54]

-----<<< Figure 4 >>>-----

PL Quenching of Blend Films. As illustrated in Figure 5, and tabulated in Table 4, the inclusion of 5 wt% PCBM in the spin-coating solutions resulted in efficient polymer emission quenching (Q_e of 70 – 90%) for all the polythiophenes studied herein. In contrast to our recent study of emission quenching in a polyfluorene/PCBM blend film,[39] with the exception of P(T_{12}NpT_{12}), no PCBM singlet emission (λ_{max} ~ 700 nm) was observed for any of the blend films studied here. Similarly no evidence could be obtained for the appearance of any other lower energy emission bands analogous to the 'exciplex' emission reported for PPV-based films. For P(T_{12}NpT_{12}) / PCBM blend films, a weak 700 nm band was observed for the blend film not

present for the pristine film, indicative of singlet energy transfer from P(T_{12}NpT_{12}) to PCBM. This observation is consistent with this polymer exhibiting the relatively blue shifted PL maximum of this polymer, resulting in enhanced spectral overlap with PCBM absorption. The efficient polythiophene emission quenching observed for all blend films indicates good blending of polymer and PCBM species, such that exciton diffusion to the polymer/PCBM interface is not a limiting factor for any of the polymers studied herein.

-----<<< Figure 5 >>>-----

-----<<< Table 4 >>>-----

Transient Absorption of Blend Films. Figure 6(a) shows transient absorption spectra of the amorphous P(T_{10}PhT_{10})/PCBM blend film. The spectrum at 10 μs exhibited an absorption peak around 700 nm, similar to that observed for the P(T_{10}PhT_{10}) pristine film as shown in Figure 2. However in contrast to the pristine film, the shape of the transient spectrum varied with time, with the absorption peak shifting from 700 nm at 10 μs to ~ 900 nm for time delays ≥ 100 μs, demonstrating the formation of two distinct transient species in the blend film. The time evolution of the transient signal ΔOD at 700 nm was well fitted with a sum of a single exponential function and a power equation: $\Delta OD = A \exp(-t/\tau) + B\, t^{-\alpha}$. The monoexponential lifetime was $\tau = 8$ μs under Ar atmosphere and significantly shortened under O_2 atmosphere, similar with the lifetimes of the ^{3}P* formed in the P(T_{10}PhT_{10}) pristine film. This fast, monoexponential phase is therefore assigned to the decay of P(T_{10}PhT_{10}) triplet excitons. Remarkably the magnitude of this initial triplet signal (see Figure 6b) is not significantly

quenched in the blend compared to the pristine film, despite the strong emission quenching. The power-law decay is characteristic of the bimolecular charge recombination of long-lived, dissociated charged species.[55,56] The exponent in the power equation was $\alpha = 0.3$, which is similar to that reported for the poly(2-methoxy-5-(3',7'-dimethyloctyloxy)-*p*-phenylenevinylene) (MDMO-PPV) and PCBM blend system.[57] The sub-unity value for α (α would be expected to equal 1 for ideal bimolecular recombination) has been discussed previously in terms of polaron trapping in a distribution of energetic traps in the polymer.[55–57] Indistinguishable power-law decay dynamics were observed under O_2 atmosphere, confirming that this power-law decay cannot be assigned to triplet excitons. We note however that the amplitude of this power-law transient decreased by ~ 30% under the O_2 atmosphere. This indicates a reduction in the yield of charge separated polarons under the O_2 atmosphere. The significance of this observation will be discussed below.

Analogous transient absorption data were obtained for the other amorphous polymer/PCBM blend films, although the magnitudes of the triplet and polaron transient absorption signals varied significantly between polymers. For the P(T_{12}NpT_{12})/PCBM blend film, PCBM triplet rather than polymer triplet formation was observed.[37] As we have discussed in reference 37, the high polymer/PCBM triplet yields observed for these blend films, in conjunction with the strong emission quenching, indicate that the triplet states do not originate from direct intersystem crossing from the polymer singlet exciton. They are assigned instead to the products of geminate recombination of triplet BRP states. A detailed model for this behavior is discussed below. For both the P(T_{12}NpT_{12}) and P($T_8T_8T_0$) blend films, the amplitude of the power-law decay assigned to dissociated polarons was an order of magnitude lower than for the P(T_{10}PhT_{10}) blend films, as detailed in Table 4, and indicative of large

differences in polaron generation yield between the three polymers.

-----<<< Figure 6 >>>-----

Turning now to the more crystalline polymers, P($T_0T_0TT_{16}$)/PCBM blend films exhibited a broad transient absorption signal around 900 – 1000 nm, similar to, but significantly enhanced in amplitude, from that observed for the P($T_0T_0TT_{16}$) pristine film. As shown in Figure 7, this initial transient absorption decayed rapidly in less than 1 μs and left a residual long-lived transient which extended up to milliseconds. This suggests that there are two independent transient species. The transient decay at 960 nm could be approximately fitted with a sum of a single exponential function and a power equation: $\Delta OD = A \exp(-t/\tau) + B\, t^{-\alpha}$. From the fitting, the lifetime τ and the exponent α were evaluated to be $\tau \sim 0.1$ μs and $\alpha = 0.4$, respectively, suggesting that there are two independent decay pathways. As shown in Figure 7, no changes in the decay dynamics were observed under O_2 atmosphere. Thus, neither of these transient species can be assigned to triplet excitons.

Blend films for the other more crystalline polymers P($T_{12}T_{12}TT_0$), P(T_0TT_{16}), and P($T_{12}SeT_{12}$) all exhibit biphasic decays analogous to those shown for the P($T_0T_0TT_{16}$)/PCBM blend film. The amplitude of the power-law decay phase which is assigned to dissociated polarons varied by an order of magnitude between polymers, as tabulated in Table 4, and indicates large variations in charge dissociation yields between these polymers.

-----<<< Figure 7 >>>-----

As shown in Figure 8, the P3HT/PCBM blend film exhibits the largest transient absorption signal of the blend films investigated in this paper. The transient spectrum exhibits a broad transient absorption signal over the wavelength range studied with an absorption maximum at ~ 1020 nm. Decays measured at 700 and 1000 nm obeyed a power law over the entire measured time range and were well fitted with a single power-law component with an exponent α = 0.7, suggesting that there is only one decay process in the blend film. Furthermore, the transient signal was not quenched under O_2 atmosphere. Therefore, the decay was assigned to the bimolecular recombination of charged species trapped in the blend films, as we have discussed previously. We note that the exponent of $\alpha = 0.7$ is much larger than that reported for other polymer/PCBM blend films, including P3HT/PCBM films at higher PCBM concentrations[17,57,58] and approaches the value of unity corresponding to trap-free (non-dispersive) bimolecular charge recombination. Thus, the large exponent suggests that there are less or shallower trap sites in the P3HT/PCBM compared with other blend films. The fitting parameters obtained are summarized in Table 4.

-----<<< Figure 8 >>>-----

The amplitude of the power-law decays varied sub-linearly with excitation density (see supporting information) for all the polymer/PCBM films studied, as we have reported previously for MDMO-PPV/PCBM blends.[58] This sub-linear behavior has been assigned to the effects of trap filling.[58] However the variation of power-law amplitude between polymers was maintained for all excitation densities, with in fact the largest variation being observed at low excitation densities (for reasons of signal to noise, the data shown in Table 4 were obtained for excitation

densities in the range 20 – 50 μJ cm^{-2}).

The key parameter of this investigation that is likely to impact PV device performance is the yield of long-lived, dissociated polarons which are required for photocurrent generation. The yield of these polarons (η_{CS}) can be most readily quantified by the amplitude of the power-law decay assigned to the bimolecular recombination of these dissociated charges. Figure 9 shows a graph of the ΔOD amplitude of this power-law transient absorbance plotted against the polymer IP for the blend films, monitored at 1 μs and a probe wavelength of 1000 nm. The amplitude has been normalized for variations in the optical densities between blend films. The amplitude at 1 μs was obtained where necessary by extrapolation from the power-law decay observed at the longer time delays to avoid contribution to the signal from triplet excitons. The 1-μs time delay was selected to be on the same timescale as charge collection in P3HT/PCBM PV cells.[59] The probe wavelength was selected to correspond to approximately the polaron absorption maximum for the films studied, with contributions from both PCBM anion and polymer cation. It is remarkable that, despite similar emission quenching for all seven polymers, the yield of this transient absorption signal assigned to long-lived polarons varies by over two orders of magnitude between polymer blends studied. This range is much greater than any residual uncertainties (for example variations in P^+ extinction coefficient) in relating this ΔOD signal magnitude to charge generation yield and therefore strongly indicates large variations in charge generation yield, η_{CS}, within this polymer series. P3HT/PCBM blend films exhibited the highest yield of long-lived polarons, consistent with its well documented efficient device performance. More surprisingly, no correlation is apparent between ΔOD signal magnitude and IP for all the polymers used in this study. It is furthermore apparent that the charge generation yield does not correlate strongly with polymer crystallinity, with the amorphous polymers

exhibiting a similar range of charge generation yields to the more crystalline polymers. In contrast, further analyses based upon estimates of the free energy difference for charge separation do indicate a significant correlation with charge generation yield, as we discuss in detail below.

-----<<< Figure 9 >>>-----

Discussion

We first consider the fundamental photophysics and photochemistry of the polymer films addressed in this study, before moving onto consideration of the relevance of these observations to PV device performance.

Photophysical Characterization of Pristine Films. We start off our discussion by considering the difference between the photophysics of the amorphous pristine polymer films $P(T_{10}PhT_{10})$, $P(T_{12}NpT_{12})$, and $P(T_8T_8T_0)$, with that of the more crystalline polymers $P(T_{12}T_{12}TT_0)$, $P(T_0T_0TT_{16})$, $P(T_0TT_{16})$, $P(T_{12}SeT_{12})$, and P3HT. For the pristine amorphous polymer films, triplet excitons were observed as the main transient species generated by optical excitation, with a lifetime of several microseconds. For the more crystalline polymers, on the other hand, short-lived (< 1 μs) polarons were observed as the main transient species. Herein we discuss the difference in the transient species on the basis of the molecular structure of the main chain of the polymers as illustrated in Figure 2.

The amorphous morphology of the first polymer group is attributed to their twisted backbones which results in a short conjugation length of the main chain, consistent with the blue-

shifted absorption band, larger IP, and low carrier mobility. Shorter conjugation lengths are likely to result in more localized excitons, consistent with the larger Stokes shift ΔE_{Stokes}. This increased exciton localization is likely to result in a larger energy gap between the lowest singlet and triplet excitons ΔE_{ST}.[60,61] As a result, triplet excitons can be expected to be the lowest excited state to which photoexcitations can finally relax. Furthermore, the twisted conjugated backbone may enhance the intersystem crossing rate between singlet and triplet excitons; correlated quantum-chemical calculations have demonstrated that the spin–orbit coupling in oligothiophenes increases with increase in the twist angle between adjacent thiophene rings.[62] Thus, we conclude that the efficient triplet formation observed here for the more amorphous polymers is attributable to the twisted backbone of the amorphous polymers.

On the other hand, the higher crystallinity of the second polymer group is attributed to their relatively planar backbones, resulting in a longer conjugation length of the main chain. This is consistent with the red-shifted absorption band, smaller IP, and high carrier mobility. In contrast to the amorphous polymers, excitons will be more delocalized in the partially crystalline polymers, consistent with the smaller ΔE_{Stokes} and indicative of a smaller singlet–triplet exciton energy separation ΔE_{ST}. Furthermore, the planar conjugated backbone, favoring interplanar interaction leading to π stacking in the conjugated backbone, can be expected to reduce the intersystem crossing rate between singlet and triplet excitons. This π-stacking structure can be expected to reduce this intersystem crossing rate as twist motions enhancing the spin–orbit coupling are effectively suppressed in the π-stacked main chain. Indeed, no triplet formation has been observed in a highly ordered regioregular P3HT film.[53] Rather, such π stacking can be expected to favor interchain charge separation, consistent with the low PL intensity and the transient absorption data reported here and with previous reports of polaron generation in pristine

regioregular P3HT films.[53] We note that the short lifetime of the photogenerated charges in these pristine films suggests that these charges most probably decay via geminate rather than bimolecular recombination. The small transient signals observed are indicative of rapid geminate recombination within the instrumental response function.

Photophysical Processes in Amorphous Blend Films. In this study, the low PCBM concentration employed in the blend films allows us to assume that the initial photogenerated excited state in these films is still the polymer singlet exciton $^1P^*$ (the PCBM exhibiting negligible absorption at the excitation wavelength). The efficient emission quenching observed for all blend films allows us to conclude that the $^1P^*$ states are efficiently quenched by the addition of only 5 wt% PCBM to the polymer film. As such, our discussion focuses not on the diffusion of excitons to the polymer/PCBM interface, but rather upon the efficiency of charge photogeneration once excitons reach this interface. The addition of this low concentration of PCBM is unlikely to alter the intersystem crossing or internal conversion decay rates from the $^1P^*$ states, consistent with there being no measurable change in polymer absorption spectra. Rather this emission quenching is assigned to the generation of polarons, P^+ and $PCBM^-$. From the data we have obtained, we are unable to distinguish between direct charge separation from the $^1P^*$ and Förster energy transfer from $^1P^*$ to $^1PCBM^*$ (see reference 39) followed by charge separation from the PCBM singlet state. However we note that, except for the $P(T_{12}NpT_{12})$/PCBM blend film, the absence of any detectable $^1PCBM^*$ emission indicates that any $^1PCBM^*$ states formed by such energy transfer are rapidly quenched by charge separation from this state. We furthermore note that the relatively low PL yields for polythiophenes such as those studied here suggest that energy transfer from $^1P^*$ to $^1PCBM^*$ is likely to be less

efficient for this polymer class compared to other more emissive polymers such polyfluorenes.[39] In either case, the emission quenching is attributed to the generation of a high yield of charged species, P^+ and $PCBM^-$.

-----<<< Scheme 1 >>>-----

We turn now to consideration of the energetics of the exciton and polaron states in these polymer blend films. For the amorphous polymers, as mentioned before, the $^1P^*$ energy, E_S, estimated from the absorption and emission spectra, is 2.5 – 2.7 eV above the ground state. For these polymers, the triplet energy level E_T of $^3P^*$ is estimated to be in the range 1 – 1.7 eV, assuming a value for ΔE_{ST} close to that of oligothiophenes (1 – 1.5 eV)[60] compatible with their short conjugation length. Similar values of ΔE_{ST} have been reported for various conjugated polymers except for a ladder-type polyfluorene (MeLPPP) with rigid and planar backbone structures.[63] For the polymers $P(T_{10}PhT_{10})$ and $P(T_8T_8T_0)$, our observation of polymer triplet formation in the blend films indicates that their triplet energies are below that of PCBM ($E_T \sim 1.5$ eV),[64,65] whilst for $P(T_{12}NpT_{12})$, the observation of PCBM triplet rather than polymer triplet formation in the blend indicates that the $P(T_{12}NpT_{12})$ triplet state lies higher in energy than the PCBM triplet state. On the basis of the polymer IPs (Table 1) and PCBM electron affinity (EA = 3.7 eV),[66,67] the energy of the charge separation states $P^+/PCBM^-$ for these amorphous polymers can be estimated to be in the range 1.7 – 1.9 eV. Thus, we conclude that the $^3P^*/^3PCBM^*$ states are lower in energy than the charge separated states for these amorphous polymers.

The photophysical data reported herein for the polymer/fullerene blend films can be most

readily understood in terms of a two-step model for charge dissociation, proceeding via the formation of interfacial BRP state, analogous to recent models proposed for polymer/polymer blend films based on the observation of exciplex-like emission.[29,35] Such 'intermediate' charge transfer (CT) states have also recently been reported in a photophysical study of small bandgap co-polymer blended with PCBM.[68] As we have discussed previously,[37] our observation of triplet exciton formation in the presence of quenching of singlet exciton, provides strong evidence for the relevance of this model to polythiophene/PCBM blend films. This model, for the amorphous polymers, is illustrated in Scheme 1. The initial charge separation results in the formation of a BRP state. The coulombic attraction of these BRPs (~ 100 – 400 meV depending upon estimates of the spatial separation of polarons across the polymer/PCBM interface)[69–71] results in a significant potential energy barrier to dissociation of these BRPs. We note that this charge dissociation is also associated with a significant increase in entropy (due to the large number of sites the polarons can occupy following dissociation) of similar energetic value to the coulombic attraction,[72] such that the overall thermodynamics of this dissociation may be largely neutral in terms of free energy. Following dissociation to free charge separated polarons (CS_{fr}), these polarons are trapped thermodynamically and kinetically by localization in energetic sub-band gap states (CS_{tr}), most probably resulting from local variations in polymer conformation.[21,57] Subsequent bimolecular charge recombination is kinetically limited by the kinetics of detrapping and polaron diffusion back to the polymer/PCBM interface. Scheme 1 also includes the possible presence of thermally unrelaxed BRP states (BRP*). The potential importance of such states is discussed in more detail below.

In the model illustrated in Scheme 1, the yield of dissociated polarons depends upon the kinetics of charge dissociation relative to the geminate recombination of the BRP to ground and

to the lower lying neutral triplet exciton. We note that, with favorable charge dissociation kinetics, this model predicts a significant yield of dissociated polarons, as observed for the P($T_0T_0TT_{16}$)/PCBM blend films herein, even when the neutral triplet exciton is thermodynamically lower in energy than the charge separated polarons. This situation contrasts with molecular D–A systems in solution, where rapid relaxation to the thermodynamically most stable state is typically observed, and the long-lived charge species are only observed when the systems energetics have been tuned to ensure that the charge separated states lie lower in energy than any molecular triplet states.[73–76] Our observation of long-lived charge separated states in these blend films, even when these states are thermodynamically unstable with respect to neutral triplet excitons, can be understood in terms of the kinetics of diffusion controlled bimolecular charge recombination. Polaron trapping on localized low energy trap sites within the polymer phase results in the slow decay dynamics observed for these dissociated polarons, extending up to millisecond timescales (Figure 6).

On the basis of the data presented herein, the approximate timescales of the processes determining charge photogeneration at the polymer/PCBM interface are summarized in Scheme 1. The charge separation time was estimated to be at least < 100 ps from the > 70% quenching efficiency and a luminescence lifetime of a few hundred picoseconds reported for polythiophenes.[52] This rapid charge formation is consistent with previous transient studies [JPCB 2006, 110, 25462 (P3HT/PCBM < 2.5 ps), PRB 1994, 50, 18543 (P3OT/C60 < 1 ps)]. Charge separation is assumed to result in the formation of coulombically BRP states. Subsequent decay of these BRPs in < 100 ns can either result in geminate charge recombination or charge dissociation to free charges. Geminate recombination proceeds either to the neutral triplet exciton or singlet ground state depending upon radical pair spin state. The high triplet

exciton yields observed for the blend suggests that geminate recombination proceeds primarily to the T_1 triplet exciton rather than to the S_0 singlet ground state, consistent with the expected energetic stabilization of the ^{3}BRP state relative to ^{1}BRP, and the small energy gap between the ^{3}BRP and ^{3}P* favoring a large triplet recombination rate constant.[77] On the basis of this model, our observation of large variations in the yield of long-lived polarons between different polymer blend films can be attributed to variations in the kinetic competition between geminate recombination and BRP dissociation to free charges. The origin of this variation is discussed below in terms of thermodynamics.

Our observation that the yield of long-lived polarons for the P(T_{10}PhT_{10})/PCBM blend films is quenched by ~ 30% in the presence of oxygen is of particular interest. This quenching may be due to a direct quenching of the bound radical states by molecular oxygen, although this appears unlikely due to the short lifetime of these states. More probably this quenching is associated with the observed oxygen quenching of the triplet excitons (Figures 4 and 6). As such, our observation of a reduced polaron yield in the presence of oxygen implies that recombination to the triplet exciton is reversible, with a significant probability of thermally activated charge separation from this triplet exciton back to the BRPs. A significant yield for this thermally activated pathway would be consistent with the relatively small free energy difference between the neutral triplet excitons and charge separated species estimated for the amorphous polymer series, as discussed above.

We note that the triplet and polaron formation closely related to the spin dynamics in the charge separated state as reported for several systems, including photosynthetic reaction centers,[78,79] D–A molecules,[80,81] polymer/polymer blend films.[29,35] In photosynthetic reaction centers, the back electron transfer produces a triplet state with an unusual spin polarization

showing the charge recombination within a weakly coupled, spin-correlated radical ion pair.[78,82] In D–A molecules, a triplet formation is observed following the back electron transfer.[80] The triplet formation is attributed to both S–T_0 and S–T_{-1} mixing between the radical ion pair for D–A molecules with a short separation distance because of the high value of the exchange integral J while the triplet states are formed by means of S–T_0 mixing at a long distance > 2 nm. For compact D–A dyads, long-lived intramolecular CT states have been reported and attributed to triplet CT states that do not interconvert rapidly with the corresponding singlet CT states because of a relatively large exchange interaction (e.g.: 200 – 400 cm^{-1})[83,84] between donor and acceptor in the CT states. Exchange interactions of similar magnitude can be expected for the amorphous polymer/PCBM blends reported herein, resulting in discrete ^{1}BRP and ^{3}BRP states as shown in Scheme 1.

Photophysical Processes in More Crystalline Blend Films. The absence of polymer triplet formation in the polymer/PCBM blend films formed with the more crystalline polymers can be most readily understood by consideration of the energetics of the states involved. For the more crystalline polymers, E_S was evaluated to be ~ 2.0 eV from the absorption and PL spectra. Relatively small ΔE_{ST} have been reported for conjugated polymers with planar backbone structures including highly ordered regioregular P3OT films (ΔE_{ST} = 0.45 eV)[85] and the ladder type MeLPPP in benzene solution (ΔE_{ST} = 0.54 eV).[63] Thus, the polymer triplet energy, E_T, for these polymers is estimated as ~ 1.5 eV. The energy of the charge separated states can be estimated to be in the range ~ 1.2 – 1.6 eV from IP − EA. It can thus be concluded that, in contrast to the amorphous polymers, the charge separated state are energetically likely to be more stable than the polymer and PCBM triplet states. In other words, in contrast to the amorphous

polymers, geminate recombination of ^{3}BRP states to yield neutral triplet excitons is likely to be thermodynamically unfavorable, consistent with the absence of triplet formation apparent from our transient absorption data.

-----<<< Scheme 2 >>>-----

Scheme 2 summarizes the kinetic scheme for charge photogeneration for the more crystalline polymers. Due to the relatively high energy of the triplet excitons, geminate recombination from the BRP state can only proceed to the singlet ground state. The ~ 100-ns monoexponential polaron decay phase shown in Figure 7 can be most readily assigned to decay of these BRP states. This contrasts with the amorphous blends, where the absence of such a decay phase suggests that the BRPs decay within our instrument response (< 100 ns). The longer lifetime of the BRPs for the more crystalline polymer blends is consistent with the absence of the triplet geminate recombination pathway. For these polymers, the yield of long-lived polarons will be determined by the competition between geminate recombination of BRP to ground versus charge dissociation. We note that for P3HT, the high yield of polaron generation is indicative of rapid dissociation of the BRP states, consistent with the absence of any observable geminate recombination dynamics on the timescales studied for this polymer.

Previous studies of PPV and polyfluorene-based donor/acceptor blends[29,35,36,86,87] have reported significant red-shifted exciplex-like emission and CT absorption, suggesting that the BRP states observed in these systems are radiatively coupled to the ground state. A sub-band gap absorption has also been reported for P3HT/PCBM blend films by Fourier-transform photocurrent spectroscopy.[88] This may be assigned to ground state CT absorption indicative of

the radiative coupling. However, no distinct red-shifted emission was observed up to 850 nm for the polythiophene/PCBM blends studied herein, indicating that the BRP states proposed here are not strongly radiatively coupled to the ground state. This lower radiative coupling may be associated with the relatively low emission yields of polythiophenes, with the primary decay pathways for neutral excitons of polythiophenes being non-radiative (e.g.: intersystem crossing or internal conversion to ground). Alternatively it may result from the degree of spatial overlap of the electron and hole orbitals of the radical pair (i.e.: the degree of quantum mechanical mixing of the CT and neutral exciton states). This lack of significant emission from the BRP states complicates experimental observation of these states, but is unlikely to qualitatively change their relevance to device function.

Relation between Charge Photogeneration and Device Photocurrent. As tabulated in Table 5, and illustrated in Figure 9, the yields of dissociated charges, $P^+/PCBM^-$, as measured by the amplitude of the power-law decay phases observed in the transient absorption data, vary by over two orders of magnitudes between the various polymers studied. We note that these studies were undertaken at low PCBM concentrations (5 wt%), too low for efficient PV device function. We moreover note that the amorphous polymers exhibit charge mobilities too low for efficient PV devices. Nevertheless, the variations in charge photogeneration yield reported here can reasonably be expected to an impact on device photocurrent generation. Whilst a full analysis of device behavior is beyond the scope of this paper, limited device photocurrent data were obtained, employing 1:1 blend ratios without annealing. The short-circuit photocurrents (J_{SC}) obtained are detailed in Table 4. It is apparent that for the polymers studied there is an excellent correlation between charge generation yields, η_{CS} and J_{SC}. For the amorphous

polymers, the J_{SC} of the P(T_{10}PhT_{10})/PCBM blend device was one order of magnitude larger than that of the P(T_{12}NpT_{12})/PCBM blend device, in good agreement with the variation in η_{CS} between these two polymers. For the partially crystalline polymers, the J_{SC} of the P($T_0T_0TT_{16}$)/PCBM blend device was one order of magnitude larger than that of the P($T_{12}T_{12}TT_0$)/PCBM blend device, again in good agreement with η_{CS}. The P3HT/PCBM blend films gave the highest J_{SC} and the highest value for η_{CS}. This correlation is consistent with a recent study of PPV-based polymer/polymer blends, which observed as inverse correlation between exciplex-like emission (indicative of significant geminate recombination), and PV device efficiency.[32] We note that our studies of device performance for this polymer series are relatively limited, and that other factors (blend composition, annealing, electric fields from the electrodes) are also likely to impact significantly upon device performance (see for example Ref 89). It has for example been shown that the application of electric fields can assist the dissociation of analogous, luminescence BRPs (referred to therein as 'exciplex') in polymer/polymer blend films.[30] Nevertheless it does appear that our transient absorption assay of charge photogeneration in blend films may be a useful indicator of the photocurrent generation performance of such blend films in organic PV devices.

Thermodynamic Origin of the Variation in Charge Photogeneration. At the outset of our investigation, we were expecting that the charge photogeneration yield η_{CS} would correlate either with the energetics of charge generation or with the degree of delocalization of the polymer polaron, and therefore with polymer crystallinity. As we have discussed above, we do not observe any clear correlation between charge generation yield and either polymer IP or crystallinity, as illustrated in Figure 9. Further calculations were then undertaken to estimate

the free energy difference for charge separation and evaluate its potential correlation with charge generation yield. This free energy difference ΔG_{CS}^{rel} was estimated as the difference between the singlet and triplet exciton energies (E_S or E_T) and the energy of the polaron pairs estimated as IP – EA. It should be noted that this free energy difference calculation does not take account of the coulombic attraction between the polarons (estimated to be 140 – 400 meV for the initially formed polarons, see above), and therefore should only be regarded as an indication of the relative rather than absolute magnitude of the free energy driving force for charge separation. Details of these calculations are given in the supporting information. No correlation was observed between ΔG_{CS}^{rel} and the ΔOD signal magnitude, employing either the PCBM singlet exciton energy or the PCBM or polymer triplet exciton energies. However, employing the polymer S_1 singlet exciton energies, E_S, given in Table 2, a correlation between $\Delta G_{CS}^{rel} = E_S -$ (IP − EA) and the ΔOD signal magnitude is observed, as shown in Figure 10. With the exception of the polymer, P(T_{12}NpT_{12}), it is striking that the charge separation yield appears to show correlation with ΔG_{CS}^{rel}, suggesting that the charge separation yield increases by two orders of magnitude for only a 200 meV increase in free energy driving force. The deviation for P(T_{12}NpT_{12}) is attributed to energy transfer from ^{1}P* to ^{1}PCBM* lowering the effective energy of the singlet exciton, and therefore the effective ΔG_{CS}^{rel} consistent with our observation of PCBM singlet exciton emission for P(T_{12}NpT_{12}) / PCBM blend films.

-----<<< Figure 10 >>>-----

The correlation between ΔG_{CS}^{rel} and the yield of long-lived, dissociated polarons contrasts with the lack of variation of exciton PL quenching between the different polymers. This

observation strongly indicates the observed dependence of charge generation upon ΔG_{CS}^{rel} does not result directly from the efficiency of exciton quenching at the polymer/PCBM interface. Rather it suggests that the efficiency of dissociation of initially formed BRPs is dependent upon ΔG_{CS}^{rel}. This observation can potentially be rationalized in terms of a model proposed by Friend and co-workers for charge dissociation in polymer/polymer blends.[30] In their paper, it was proposed that exciton quenching at the donor/acceptor interface initially formed a thermally 'hot' BRP state (BRP* in Schemes 1 and 2). This thermally hot radical pair has a high probability of dissociation into free polarons. This dissociation however competes with thermal relaxation of the BRP. Once thermally relaxed, the BRP has insufficient energy to overcome the coulombic attraction of the polarons, but rather primarily undergoes geminate recombination. Within this model, the free energy of charge separation, ΔG_{CS}^{rel}, will influence the extent to which the initially formed BRP is indeed thermally 'hot' (with a large ΔG_{CS}^{rel} corresponding to more thermal energy in the initially formed BRPs), and could thereby provide a physical mechanism to explain the dependence of the yield of dissociated charges upon ΔG_{CS}^{rel} apparent from Figure 10. We note such a description is analogous to previous reports of 'hot' exciton dissociation in conjugated polymers.[90,91] At present, the limited data set presented herein is insufficient to provide unambiguous confirmation of the validity of this model. Nevertheless the correlation shown in Figure 10 is indicative of its potential relevance to charge generation in polymer/PCBM blend solar cells. Further experiments to test this model are currently in progress.

The subtlety of the structure–function relationship which appears to determine the charge photogeneration yield can be most clearly appreciated by consideration of the two polymers $P(T_{12}T_{12}TT_0)$ and $P(T_0T_0TT_{16})$. When blended with 5 wt% PCBM, the polymer luminescence is

quenched in both cases by 75 – 80%. These two polymers have identical polymer backbones and differ only in the location and length of their alkyl sidechains. MOPAC-AM2 calculations for these polymers indicated a slightly more planar backbone configuration for $P(T_0T_0TT_{16})$ compared to $P(T_{12}T_{12}TT_0)$. They are synthesized by similar synthetic strategies. They exhibit similar charge carrier mobilities and IPs. They differ only in a small red-shift of the absorption and PL bands of $P(T_{12}T_{12}TT_0)$, corresponding to a ~ 0.1 eV shift in the energy of their singlet excitons. Despite these similarities, their charge photogeneration yields in the blend with 5 wt% PCBM differs by over an order of magnitude. This difference in charge photogeneration yield was found to be reproducible between different polymer batches. Further studies of the $P(T_nT_nTT_0)$ polymer series for alkyl chain lengths up to 16 observed no significant dependence of charge generation yield upon alkyl chain length (data not shown). Rather it seems more likely that this difference in charge generation performance derives either from the small difference in singlet exciton energy, and its resultant influence upon the free energy of charge separation or upon some residual dependence of backbone planarity.

Conclusions

The most striking conclusion from this study is that, despite the efficient PL quenching observed for all the polythiophene/PCBM blends studied, the yield of long-lived, dissociated polarons varies by two orders of magnitude depending upon the polythiophene employed. This observation clearly indicates PL quenching is not a reliable indicator of dissociated charge generation in such blend films. This observation can be most readily rationalized in terms of a two-step model for charge dissociation. Exciton quenching at the polymer/PCBM interface

initially results in the generation of coulombically BRP states analogous to the exciplex-like states reported previously for PPV-based blend films. Dissociation of these BRPs is in kinetic competition with their geminate recombination either to ground or to neutral triplet excitons. This model is in particular supported by our observations of high polymer and PCBM triplet yields in the blend films. The strong quenching of the polymer singlet exciton emission, and the lack of observation of any PCBM emission, strongly indicate that these triplets cannot originate from intersystem crossing from singlet excitons, but rather from geminate recombination from triplet BRP states. Oxygen dependence studies furthermore indicate that this geminate recombination pathway to triplet excitons is reversible, consistent with our estimates of only small free energy change for this recombination reaction. The large variation in charge generation yield between the different polythiophenes appears to correlate with estimates of the energy difference ΔG_{CS}^{rel} between the polymer singlet exciton E_S and the dissociated polarons (as given by IP − EA). This correlation can be most readily understood in terms of the efficiency of dissociation of the BRPs being dependent upon the thermal energy of the initially formed BRPs, with a large ΔG_{CS}^{rel} resulting in the initially formed BRPs being thermally hotter, and therefore exhibiting a higher charge dissociation yield. These observations suggest that, at least for the polythiophene / PCBM blend films studied herein, the minimum free energy difference required to achieve efficient charge dissociation is significantly larger than that required to achieve exciton quenching at the polymer / PCBM interface. This in turn has important implications for energy level requirements, and specifically LUMO level offset, required to achieve further advances in photovoltaic device performance.

Acknowledgments. We thank Jessica J. Benson-Smith for helpful discussions and Dr Tracey Clarke for assistance with the PL data for P(T_{12}NpT_{12}). This work was supported by DTI technology program renewable energy polymer photovoltaics project. H.O. is grateful for support from Science Exchange Program between the Japan Society for the Promotion of Science (JSPS) and the Royal Society.

Supporting Information Available: Details about X-ray diffraction measurements of some pristine films, intensity dependence of transient absorption decays for P(T_{10}PhT_{10})/PCBM, P($T_0T_0TT_{16}$)/PCBM, and P3HT/PCBM blend films, calculations of the free energy difference $-\Delta G_{CS}^{rel}$, dependence of the ΔOD signal magnitude on $-\Delta G_{CS}^{rel}$ employing either the PCBM singlet exciton energy or the PCBM or polymer triplet exciton energies, and a full list of authors for reference 1. This material is available free of charge via the Internet at http://pubs.acs.org.

References and Footnotes

[†] Department of Chemistry, Imperial College London

[‡] Merck Chemicals

[§] Department of Physics, Imperial College London

[#] Present address: Department of Polymer Chemistry, Graduate School of Engineering, Kyoto University, Katsura, Nishikyo, Kyoto 615-8510, Japan

[‖] Present address: Department of Materials, School of Engineering and Materials Science, Queen Mary, University of London, Mile End Road, London E1 4NS, United Kingdom

[⊥] Present address: Department of Chemistry, Imperial College London, Exhibition Road, London SW7 2AZ, United Kingdom

(1) Adams, D. M. et al. *J. Phys. Chem. B* **2003**, *107*, 6668–6697.

(2) Barbara, P. F.; Meyer, T. J.; Ratner, M. A. *J. Phys. Chem.* **1996**, *100*, 13148–13168.

(3) Marcus, R. A.; Sutin, N. *Biochim. Biophys. Acta* **1985**, *811*, 265–322.

(4) Miller, J. R.; Calcatterra, L. T.; Closs, G. L. *J. Am. Chem. Soc.* **1984**, *106*, 3047–3049.

(5) Asahi, T.; Ohkohchi, M.; Matsusaka, R.; Mataga, N.; Zhang, R. P.; Osuka, A.; Maruyama, K. *J. Am. Chem. Soc.* **1993**, *115*, 5665–5674.

(6) Wasielewski, M. R. *Chem. Rev.* **1992**, *92*, 435–461.

(7) Gust, D.; Moore, T. A.; Moore, A. L. *Acc. Chem. Res.* **2001**, *34*, 40–48.

(8) Fukuzumi, S. *Bull. Chem. Soc. Jpn.* **2006**, *79*, 177–195.

(9) Verhoeven, J. W. *J. Photochem. Photobiol. C: Photochem. Rev.* **2006**, *7*, 40–60.

(10) Verhoeven, J. W.; van Ramesdonk, H. J.; Groeneveld, M. M.; Benniston, A. C.; Harriman, A. *ChemPhysChem* **2005**, *6*, 2251–2260.

(11) Morita, S.; Zakhidov, A. A.; Yoshino, K. *Solid State Commun.* **1992**, *82*, 249–252.

(12) Smilowitz, L.; Sariciftci, N. S.; Wu, R.; Gettinger, C.; Heeger, A. J.; Wudl, F. *Phys. Rev. B* **1993**, *47*, 13835–13842.

(13) Brabec, C. J.; Sariciftci, N. S.; Hummelen, J. C. *Adv. Mater. Funct.* **2001**, *11*, 15–26.

(14) Reyes-Reyes, M.; Kim, K.; Carroll, D. L. *Appl. Phys. Lett.* **2005**, *87*, 083506.

(15) Ma, W.; Yang, C.; Gong, X.; Lee, K.; Heeger, A. J. *Adv. Funct. Mater.* **2005**, *15*, 1617–1622.

(16) Li, G.; Shrotriya, V.; Huang, J.; Yao, Y.; Moriarty, T.; Emery, K.; Yang, Y. *Nature Mater.* **2005**, *4*, 864–868.

(17) Kim, Y.; Cook, S.; Tuladhar, S. M.; Choulis, S. A.; Nelson, J.; Durrant, J. R.; Bradley, D. D. C.; Giles, M.; McCulloch, I.; Ha, C. -S.; Ree, M. *Nature Mater.* **2006**, *5*, 197–203.

(18) Kim, J. Y.; Kim, S. H.; Lee, H. -H.; Lee, K.; Ma, W.; Gong, X.; Heeger, A. J. *Adv. Mater.* **2006**, *18*, 572–576.

(19) Kim, K.; Liu, J.; Namboothiry, M. A. G.; Carroll, D. L. *Appl. Phys. Lett.* **2007**, *90*, 163511.

(20) Padinger, F.; Rittberger, R. S.; Sariciftci, N. S. *Adv. Funct. Mater.* **2003**, *13*, 85–88.

(21) Kim, Y.; Choulis, S. A.; Nelson, J.; Bradley, D. D. C.; Cook, S.; Durrant, J. R. *J. Mater. Sci.* **2005**, *40*, 1371–1376.

(22) Nakamura, J.; Murata, K.; Takahashi, K. *Appl. Phys. Lett.* **2005**, *87*, 132105.

(23) Al-Ibrahim, M.; Ambacher, O.; Sensfuss, S.; Gobsch, G. *Appl. Phys. Lett.* **2005**, *86*, 201120.

(24) Li, G.; Shrotriya, V.; Yao, Y.; Yang, Y. *J. Appl. Phys.* **2005**, *98*, 043704.

(25) Hiorns, R. C.; de Bettignies, R.; Leroy, J.; Bailly, S.; Firon, M.; Sentein, C.; Khoukh, A.; Preud'homme, H.; Dagron-Lartigau, C. *Adv. Funct. Mater.* **2006**, *16*, 2263–2273.

(26) Scharber, M. C.; Mühlbacher, D.; Koppe, M.; Denk, P.; Waldauf, C.; Heeger, A. J.; Brabec, C. J. *Adv. Mater.* **2006**, *18*, 789–794.

(27) Kooistra, F. B.; Knol, J.; Kastenberg, F.; Popescu, L. M.; Verhees, W. J. H.; Kroon, J. M.; Hummelen, J. C. *Org. Lett.* **2007**, *9*, 551–554.

(28) Müller, J. G.; Lupton, J. M.; Feldmann, J.; Lemmer, U.; Schaber, M. C.; Sariciftci, N. S.; Brabec, C. J.; Scherf, U. *Phys. Rev. B* **2005**, *72*, 195208.

(29) Offermans, T.; van Hal, P. A.; Meskers, S. C. J.; Koetse, M. M.; Janssen, R. A. J. *Phys. Rev. B* **2005**, *72*, 045213.

(30) Morteani, A. C.; Sreearunothai, P.; Herz, L. M.; Friend, R. H.; Silva, C. *Phys. Rev. Lett.* **2004**, *92*, 247402.

(31) Yin, C.; Kietzke, T.; Kumke, M.; Neher, D.; Hörhold, H. -H. *Sol. Energy Mater. Sol. Cells* **2007**, *91*, 411–415.

(32) Yin, C.; Kietzke, T.; Neher, D.; Hörhold, H. -H. *Appl. Phys. Lett.* **2007**, *90*, 092117.

(33) The term ‘exciplex’ was originally employed in photochemical studies to refer the formation of an excited state molecular complex — observed in systems where optical excitation of monomeric molecular species was observed to result in the formation of molecular dimers (See ref 34). As such, the use of this term for solid state molecular

system where optical excitation does not result in a significant change in donor–acceptor spatial separation is rather questionable.

(34) Birks, J. B. *Photophysics of Aromatic Molecules*; Wiley-Interscience: London, UK, 1970; Chapter 9.

(35) Ford, T. A.; Avilov, I.; Beljonne, D.; Greenham, N. C. *Phys. Rev. B* **2005**, *71*, 125212.

(36) Benson-Smith, J. J.; Goris, L.; Vandewal, K.; Haenen, K.; Manca, J. V.; Vanderzande, D.; Bradley, D. D. C.; Nelson, J. *Adv. Funct. Mater.* **2007**, *17*, 451–457.

(37) Ohkita, H.; Cook, S.; Astuti, Y.; Duffy, W.; Heeney, M.; Tierney, S.; McCulloch, I.; Bradley, D. D. C.; Durrant, J. R. *Chem. Commun.* **2006**, 3939–3941.

(38) Veldman, D.; Offermans, T.; Sweelssen, J.; Koetse, M. M.; Meskers, S. C. J.; Janssen, R. A. J. *Thin. Solid Films* **2006**, *511–512*, 333–337.

(39) Cook, S.; Ohkita, H.; Durrant, J. R.; Kim, Y.; Benson-Smith, J. J.; Nelson, J.; Bradley, D. D. C. *Appl. Phys. Lett.* **2006**, *89*, 101128.

(40) Veldman, D.; Bastiaansen, J. J. A. M.; Langeveld-Voss, B. M. W.; Sweelssen, J.; Koetse, M. M.; Meskers, S. C. J.; Janssen, R. A. J. *Thin. Solid Films* **2006**, *511–512*, 581–586.

(41) McCulloch, I.; Bailey, C.; Giles, M.; Heeney, M.; Love, I.; Shkunov, M.; Sparrowe, D.; Tierney, S. *Chem. Mater*. **2005**, *17*, 1381–1385.

(42) Tierney, S.; Heeney, M.; McCulloch, I. *Synth. Met.* **2005**, *148*, 195–198.

(43) Heeney, M.; Bailey, C.; Genevicius, K.; Shkunov, M.; Sparrowe, D.; Tierney, S.; McCulloch, I. *J. Am. Chem. Soc.* **2005**, *127*, 1078–1079.

(44) McCulloch, I.; Heeney, M.; Bailey, C.; Genevicius, K.; MacDonald, I.; Shkunov, M.; Sparrowe, D.; Tierney, S.; Wagner, R.; Zhang, W.; Chabinyc, M. L.; Kline, R. J.; McGehee, M. D.; Toney, M. F. *Nature Mater*. **2006**, *5*, 328–333.

(45) DeLongchamp, D. M.; Kline, R. J.; Lin, E. K.; Fischer, D. A.; Richter, L. J.; Lucas, L. A.; Heeney, M.; McCulloch, I.; Northrup, J. E. *Adv. Mater.* **2007**, *19*, 833–837.

(46) Hummelen, J. C.; Knight B. W.; LePeq, F.; Wudl, F.; Yao, J.; Wilkins, C. L. *J. Org. Chem.* **1995**, *60*, 532–538.

(47) Ohkita, H.; Cook, S.; Ford, T. A.; Greenham, N. C.; Durrant, J. R. *J. Photochem. Photobiol. A: Chem.* **2006**, *182*, 225–230.

(48) Cornil, J.; Beljonne, D.; Calbert, J. -P.; Brédas, J. -L. *Adv. Mater.* **2001**, *13*, 1053–1067.

(49) Gierschner, J.; Cornil, J.; Egelhaaf, H. -J. *Adv. Mater.* **2007**, *19*, 1–20.

(50) Chen, T. -A.; Wu, X.; Rieke, R. D. *J. Am. Chem. Soc.* **1995**, *117*, 233–244.

(51) Kraabel, B.; Moses, D.; Heeger, A. J. *J. Chem. Phys.* **1995**, *103*, 5102–5108.

(52) Kim, Y.; Bradley, D. D. C. *Curr. Appl. Phys.* **2005**, *5*, 222–226.

(53) Korovyanko, O. J.; Österbacka, R.; Jiang, X. M.; Vardeny, Z. V.; Janssen, R. A. J. *Phys. Rev. B* **2001**, *64*, 235122.

(54) Cook, S. *Ph.D. Thesis*, Imperial College London, London, **2006**.

(55) Nelson, J. *Phys. Rev. B* **2003**, *67*, 155209.

(56) Nelson, J.; Choulis, S. A.; Durrant, J. R. *Thin Solid Films* **2004**, *451–452*, 508–514.

(57) Nogueira, A. F.; Montanari, I.; Nelson, J.; Durrant, J. R.; Winder, C.; Sariciftci, N. S.; Brabec, C. *J. Phys. Chem. B* **2003**, *107*, 1567–1573.

(58) Montanari, I.; Fogueira, A. F.; Nelson, J.; Durrant, J. R.; Winder, C.; Loi, M. A.; Sariciftci, N. S.; Brabec, C. *Appl. Phys. Lett.* **2002**, *81*, 3001–3003.

(59) Shuttle, C.; O'Regan, B. C.; Durrant, J. R. unpublished.

(60) Seixas de Melo, J.; Silva, L. M.; Arnaut, L. G.; Becker, R. S. *J. Chem. Phys.* **1999**, *111*, 5427–5433.

(61) Scholes, G. D.; Rumbles, G. *Nature Mater.* **2006**, *5*, 683–696.

(62) Beljonne, D.; Shuai, Z.; Pourtois, G.; Bredas, J. L. *J. Phys. Chem. A* **2001**, *105*, 3899–3907.

(63) Monkman, A.; Burrows, H. D. *Synth. Met.* **2004**, *141*, 81–86.

(64) Williams, R. M.; Zwier, J. M.; Verhoeven, J. W. *J. Am. Chem. Soc.* **1995**, *117*, 4093–4099.

(65) Guldi, D. M.; Hungerbühler, H.; Carmichael, I.; Asmus, K. -D.; Maggini, M. *J. Phys. Chem. A* **2000**, *104*, 8601–8608.

(66) Brabec, C. J.; Cravino, A.; Meissner, D.; Sariciftci, N. S.; Fromherz, T.; Rispens, M. T.; Sanchez, L.; Hummelen, J. C. *Adv. Funct. Mater.* **2001**, *11*, 374–380.

(67) Mihailetchi, V. D.; Blom, P. W. M.; Hummelen, J. C.; Rispens, M. T. *J. Appl. Phys.* **2003**, *94*, 6849–6854.

(68) Hwang, I. -W.; Soci, C; Moses, D.; Zhu, Z.; Waller, D.; Gaudiana, R.; Brabec, C. J.; Heeger, A. J. *Adv. Mater.* **2007**, *19*, 2307–2312.

(69) The Coulomb binding of the initially formed BRPs can be estimated to be 410 meV, assuming a relative dielectric constant of 3.5 (an average value for P3HT, $\varepsilon = 3$ (ref 70),

and PCBM, $\varepsilon = 4.1$ (ref 71)) and spatial separation of 1 nm. Larger spatial separations of 2 or 3 nm would give binding energies of ~ 210 and 140 meV respectively.

(70) Chiguvare, Z.; Dyakonov, V. *Phys. Rev. B* **2004**, *70*, 235207.

(71) de Haas, M. P.; Warman, J. M.; Anthopoulos, T. D.; de Leeuw, D. M. *Adv. Funct. Mater.* **2006**, *16*, 2274−2280.

(72) Assuming a polaron size of 1 nm^3 and a charge density of 10^{17} cm^{-3}, the entropy contribution to the free energy of charge dissociation can be estimated to be $k_B T \ln 10^4 \sim$ 230 meV.

(73) van Hal, P. A.; Knol, J.; Langeveld-Voss, B. M. W.; Meskers, S. C. J.; Hummelen, J. C.; Janssen, R. A. J. *J. Phys. Chem. A* **2000**, *104*, 5974–5988.

(74) Luo, C.; Guldi, D. M.; Imahori, H.; Tamaki, K.; Sakata, Y. *J. Am. Chem. Soc.* **2000**, *122*, 6535–6551.

(75) Otsubo, T.; Aso, Y.; Takimiya, K. *J. Mater. Chem.* **2002**, *12*, 2565–2575.

(76) Ramos, A. M.; Meskers, S. C. J.; van Hal, P. A.; Knol, J.; Hummelen, J. C.; Janssen, R. A. J. *J. Phys. Chem. A* **2003**, *107*, 9269–9283.

(77) Mataga, N.; Chosrowjan, H.; Taniguchi, S. *J. Photochem. Photobiol. C: Photochem. Rev.* **2005**, *6*, 37–79.

(78) Dutton, P. L.; Leigh, J. S.; Seibert, M. *Biochem. Biophys. Res. Commun.* **1972**, *46*, 406–413.

(79) Rutherford, A. W.; Paterson, D. R.; Mullet, J. E. *Biochim. Biophys. Acta* **1981**, *635*, 205–214.

(80) Wiederrecht, G. P.; Svec, W. A.; Wasielewski, M. R. Galili, T.; Levanon, H. *J. Am. Soc. Chem.* **1999**, *121*, 7726–7727.

(81) Wiederrecht, G. P.; Svec, W. A.; Wasielewski, M. R. Galili, T.; Levanon, H. *J. Am. Soc. Chem.* **2000**, *122*, 9715–9722.

(82) Wasielewski, M. R. *J. Org. Chem.* **2006**, *71*, 5051–5066.

(83) Hviid, L.; Bouwman, W. G.; Paddon-Row, M. N.; van Ramesdonk, H. J.; Verhoeven, J. W.; Brouwer, A. M. *Photochem. Photobiol. Sci.* **2003**, *2*, 995–1001.

(84) Hviid, L.; Brouwer, A. M.; Paddon-Row, M. N.; Verhoeven, J. W.; *ChemPhysChem* **2001**, *2*, 232–235.

(85) Sakurai, K.; Tachibana, H.; Shiga, N.; Terakura, C.; Matsumoto, M.; Tokura, Y. *Phys. Rev. B* **1997**, *56*, 9552–9556.

(86) Hasharoni, K.; Keshavarz-K., M.; Sastre, A.; González, R.; Bellavia-Lund, C.; Greenwald, Y. *J. Chem. Phys.* **1997**, *107*, 2308–2312.

(87) Goris, L.; Haenen, K.; Nesládek, M.; Wagner, P.; Vanderzande, D.; De Schepper, L.; D'Haen, J.; Lutsen, L.; Manca, J. V. *J. Mater. Sci.* **2005**, *40*, 1413–1418.

(88) Goris, L.; Poruba, A.; Hod'ákova, L.; Vaněček, M.; Haenen, K.; Nesládek, M.; Wagner, P.; Vanderzande, D.; De Schepper, L.; Manca, J. V. *Appl. Phys. Lett.* **2006**, *88*, 052113.

(89) Koppe, M.; Scharber, M.; Brabec, C.; Duffy, W.; Heeney, M.; McCulloch, I. *Adv. Funct. Mater.* **2007**, *17*, 1371–1376.

(90) Arkhipov, V. I.; Emelianova, E. V.; Barth, S.; Bässler, H. *Phys. Rev. B* **2000**, *61*, 8207–8214.

(91) Basko, D. M.; Conwell, E. M. *Phys. Rev. B* **2002**, *66*, 155210.

CHART 1. Chemical structures of various polythiophenes with different IP. From the top: $P(T_8T_8T_0)$, $P(T_{12}NpT_{12})$, $P(T_{10}PhT_{10})$, $P(T_0T_0TT_{16})$, $P(T_{12}T_{12}TT_0)$, $P(T_{12}SeT_{12})$, $P(T_0TT_{16})$, P3HT.

Figure Captions

Figure 1. Absorption and PL spectra of P3HT (——), $P(T_0T_0TT_{16})$ (·····), and $P(T_{10}PhT_{10})$ (– – –) pristine films at room temperature.

Figure 2. Minimum-energy molecular structures calculated by the MOPAC program: a) 3-mer of $P(T_{10}PhT_{10})$, b) 2.5-mer of $P(T_0T_0TT_{16})$, c) 6-mer of P3HT.

Figure 3. Transient absorption spectra of the $P(T_{10}PhT_{10})$ pristine film at 1, 2, 3, 5, and 8 μs after the laser excitation from top to bottom. The inset shows the transient absorption decays of the $P(T_{10}PhT_{10})$ pristine film monitored at 700 nm under Ar (black line) and O_2 (gray line) atmospheres at room temperature.

Figure 4. Transient absorption spectra of the $P(T_0T_0TT_{16})$ pristine film at 0.3, 0.5, and 1 μs after the laser excitation from top to bottom. The inset shows the transient absorption decays of the $P(T_0T_0TT_{16})$ pristine film monitored at 960 nm under Ar (black line) and O_2 (gray line) atmospheres at room temperature.

Figure 5. PL spectra of $P(T_{10}PhT_{10})$/PCBM blend (solid line) and $P(T_{10}PhT_{10})$ pristine (broken line) films. The PL intensity was corrected for variation in the absorption at an

excitation wavelength of 420 nm. The PL tail of P(T_{10}PhT_{10})/PCBM blend film is multiplied by 100 (dotted line).

Figure 6. a) Transient absorption spectra of the P(T_{10}PhT_{10})/PCBM blend film at 10, 20, 100, and 800 μs after the laser excitation from top to bottom. b) Transient absorption decays of the P(T_{10}PhT_{10})/PCBM blend film monitored at 700 nm under Ar (black line) and O_2 (gray line) atmospheres at room temperature.

Figure 7. a) Transient absorption spectra of the P($T_0T_0TT_{16}$)/PCBM blend film at 0.3, 0.5, and 1 μs after the laser excitation from top to bottom. b) Transient absorption decays of the P($T_0T_0TT_{16}$)/PCBM blend film monitored at 960 nm under Ar (black line) and O_2 (gray line) atmospheres at room temperature.

Figure 8. a) Transient absorption spectra of the P3HT/PCBM blend film at 1, 2, 3, 5, and 8 μs after the laser excitation from top to bottom. b) Transient absorption decays of the P3HT/PCBM blend film monitored at 1000 nm under Ar (black line) and O_2 (gray line) atmospheres at room temperature.

Figure 9. Transient absorbance at 1 μs of the blend films plotted against polymer IPs. The absorbance was corrected for variation in the absorption at the excitation wavelength and an extrapolated value at 1 μs estimated from the power-law decay at the longer time domain, measured at a probe wavelength of 1000 nm. The open triangles and

squares represent data for the amorphous polymers and the more crystalline polymers, respectively. The arrows below data points indicate upper limit values.

Figure 10. Transient absorbance at 1 μs of the blend films plotted against $-\Delta G_{CS}^{rel}$ estimated as $E_S - (IP - EA)$ where E_S is the energy level of polymer singlet excitons. The absorbance was corrected for variation in the absorption at the excitation wavelength and an extrapolated value at 1 μs estimated from the power-law decay at the longer time domain, measured at a probe wavelength of 1000 nm. The open triangles and squares represent data for the amorphous polymers and the more crystalline polymers, respectively. The arrows below data points indicate upper limit values. The low charge generation yield for P(T_{12}NpT_{12}) is assigned to singlet energy transfer from P(T_{12}NpT_{12}) to PCBM competing effectively with charge separation.

Scheme 1. Energy diagram for charge formation via BRPs proposed for the amorphous polymer/PCBM blend films. The thick arrow from ^{3}P* represents our observation of $T_1 \rightarrow T_n$ absorption decay in transient absorption measurements. The dotted arrows represent quenching processes by oxygen molecules. The ^{1}BRP state is located slightly higher than the ^{3}BRP state because of the substantial exchange interaction 2J. The gray lines represent charge formation via 'hot' BRP state.

Scheme 2. Energy diagram for charge formation via BRPs proposed for the more crystalline

polymer/PCBM blend films. The ^{1}BRP state is in thermal equilibrium with the ^{3}BRP state. The gray lines represent charge formation via 'hot' BRP state.

TABLE 1: Characterization of Polythiophene Pristine Films

	M_w	M_n	M_w/M_n	μ [a] $cm^2 V^{-1} s^{-1}$	IP [b] eV	Crystallinity
$P(T_8T_8T_0)$	73000	29500	2.48	1×10^{-5}	5.6	amorphous
$P(T_{12}NpT_{12})$	22000	9000	2.44	6×10^{-4}	5.4	amorphous
$P(T_{10}PhT_{10})$	21900	11500	1.90	2×10^{-4}	5.4	amorphous
$P(T_0T_0TT_{16})$	98100	42000	2.34	2×10^{-1}	5.1	crystalline
$P(T_{12}T_{12}TT_0)$	51400	27900	1.84	2×10^{-1}	5.1	crystalline
$P(T_{12}SeT_{12})$	46400	23800	1.95	2×10^{-1}	5.0	crystalline
$P(T_0TT_{16})$	47600	22900	2.08	3×10^{-1}	5.0	crystalline
P3HT	20700	12400	1.67	7×10^{-3}	4.8	highly crystalline

[a] Field-effect mobility evaluated in the saturated regime.

[b] Evaluated by an ambient ultraviolet photoelectron spectroscopy technique.

TABLE 2: Photophysical Properties of Polythiophene Pristine Films

	Abs		PL		E_S	ΔE_{Stokes}
	λ_{max} / nm	λ_{0-0} [a] / nm	λ_{0-0} [a] / nm	λ_{max} / nm	eV	eV
$P(T_8T_8T_0)$	438	—	—	572	2.5 [c]	0.66 [c]
$P(T_{12}NpT_{12})$	423	—	—	519	2.7 [c]	0.54 [c]
$P(T_{10}PhT_{10})$	416	—	—	564	2.6 [c]	0.78 [c]
$P(T_0T_0TT_{16})$	531	~ 580 [b]	621	621	2.1 [d]	0.14 [d]
$P(T_{12}T_{12}TT_0)$	545	~ 595 [b]	~ 635 [b]	668	2.0 [d]	0.13 [d]
$P(T_{12}SeT_{12})$	572	618	~ 640 [b]	662	1.9 [d]	0.07 [d]
$P(T_0TT_{16})$	554	~ 595 [b]	633	663	2.1 [d]	0.13 [d]
P3HT	523	~ 600 [b]	~ 640 [b]	666	2.0 [d]	0.13 [d]

[a] λ_{0-0} represents the wavelength of the first shoulder or vibrational band in the absorption or PL spectra.

[b] Not a peak but a shoulder.

[c] Evaluated from λ_{max} of the absorption and PL spectra.

[d] Evaluated from λ_{0-0} of the absorption and PL spectra.

TABLE 3: Dihedral Angles in Oligothiophene Units Calculated by MOPAC-AM1

	Dihedral angle / deg	
	T–T [a]	T–X
$P(T_{10}PhT_{10})$	149.2	142.7 [b]
$P(T_0T_0TT_{16})$	178.9	174.1 [c]
P3HT	179.1	—

[a] Dihedral angle of neighboring two thiophene units.

[b] Dihedral angle between a 3-decythiophene unit (T_{10}) and a phenyl unit (Ph).

[c] Dihedral angle between a thiophene unit (T_0) and a 3,6-dihexadecylthieno[3,2-*b*]thiophene unit (TT_{16}).

TABLE 4: Photophysical Properties of Polythiophene/PCBM Blend Films

		Fast Phase		Slow Phase		Device Data [d]
	Q_e [a] / %	t / μs	Assignment	Amplitude [b] / $\Delta\mu$OD	α [c]	J_{SC} / mA cm^{-2}
$P(T_8T_8T_0)$	> 90	3	^{3}P*	≤ 3	0.3	0.002 [e]
$P(T_{12}NpT_{12})$	~ 80	11	^{3}PCBM*	≤ 3	0.3	—
$P(T_{10}PhT_{10})$	> 90	7	^{3}P*	90	0.3	0.02 [e]
$P(T_0T_0TT_{16})$	~ 80	~ 0.1	$P^+/PCBM^-$	30	0.4	1.8
$P(T_{12}T_{12}TT_0)$	~ 75	~ 0.1	$P^+/PCBM^-$	≤ 2	—	0.01
$P(T_{12}SeT_{12})$	~ 80	< 0.1	—	≤ 2	—	—
$P(T_0TT_{16})$	~ 70	~ 0.1	$P^+/PCBM^-$	45	0.3	—
P3HT	~ 70	—	—	160	0.7	3.4

[a] Steady-state PL quenching of the blend film relative to the corresponding pristine film.

[b] Evaluated from the amplitude of the transient absorbance power-law decay phase at 1 μs normalized by absorption at the excitation wavelength.

[c] Exponent of the power law obtained from power-law fits to this phase.

[d] Measured from bulk heterojunction organic PV devices with 1:1 blend compositions without thermal annealing. Other experimental conditions as in reference 17.

[e] Note the low hole mobilities of these amorphous polymers are expected to limit device photocurrent relative to the more crystalline materials.

P($T_8T_8T_0$)

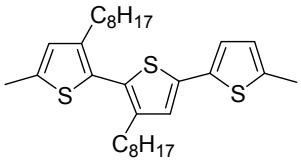

P($T_{12}NpT_{12}$)

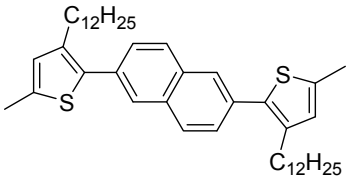

P($T_{10}PhT_{10}$)

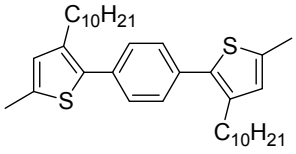

P($T_0T_0TT_{16}$)

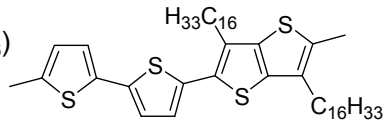

P($T_{12}T_{12}TT_0$)

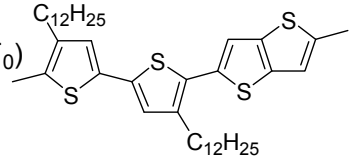

P($T_{12}SeT_{12}$)

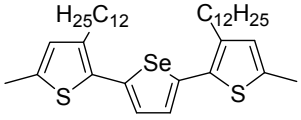

P(T_0TT_{16})

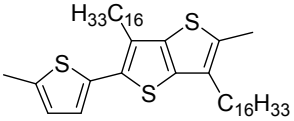

P3HT

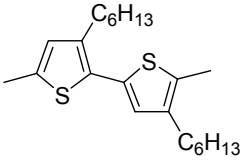

CHART 1. H. Ohkita et al.

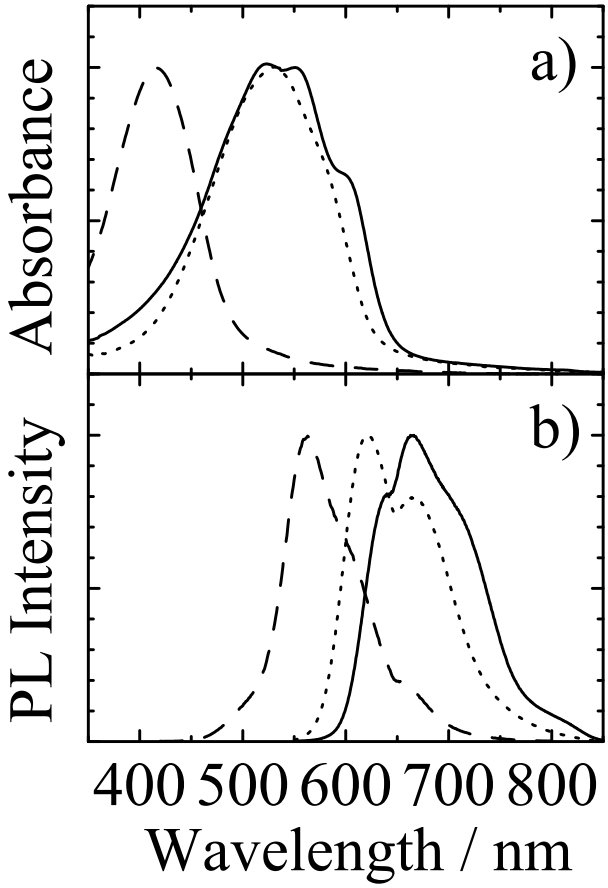

Figure 1. H. Ohkita et al.

a)

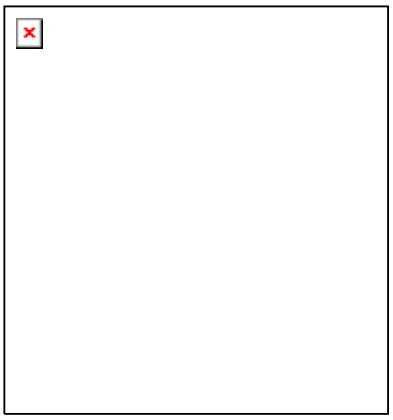

b)

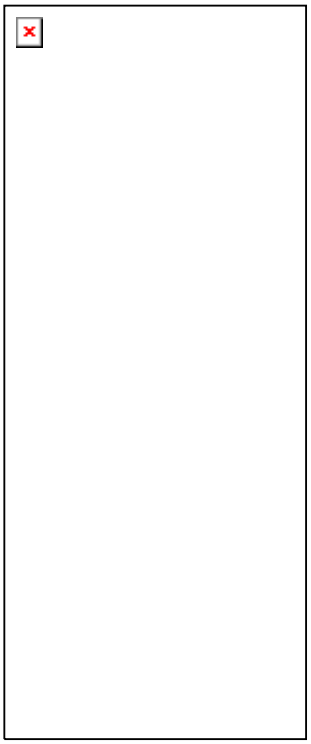

c)

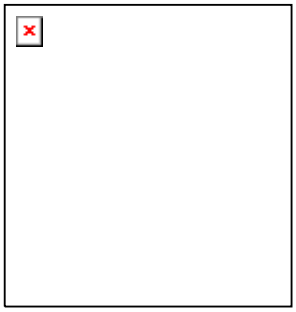

Figure 2. H. Ohkita et al.

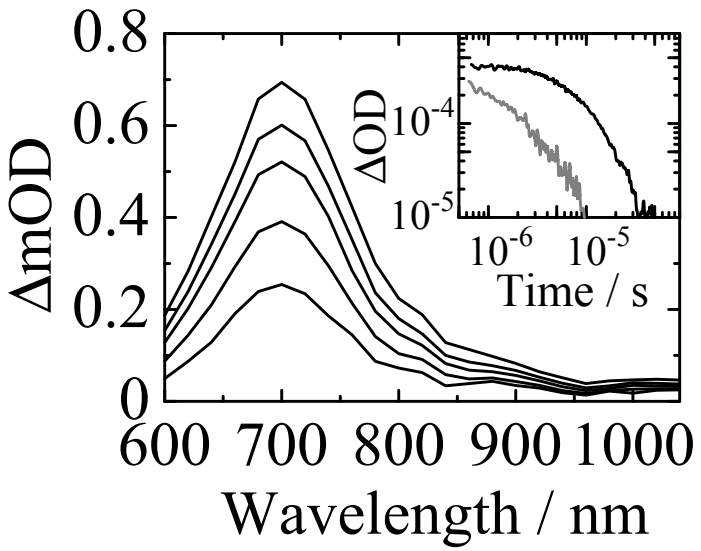

Figure 3. H. Ohkita et al.

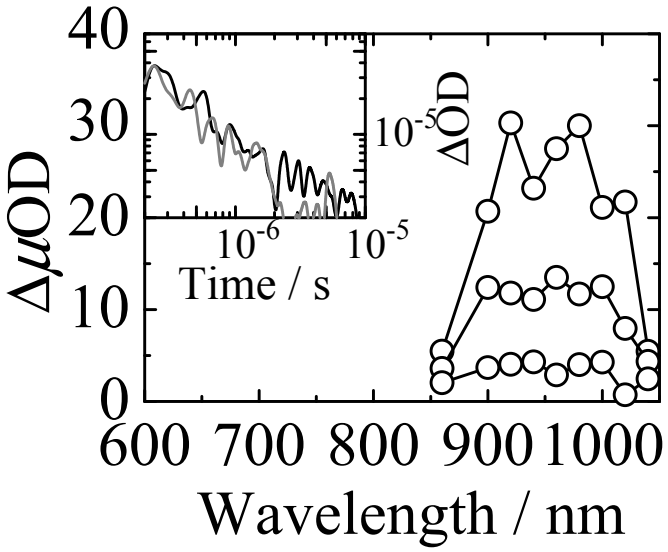

Figure 4. H. Ohkita et al.

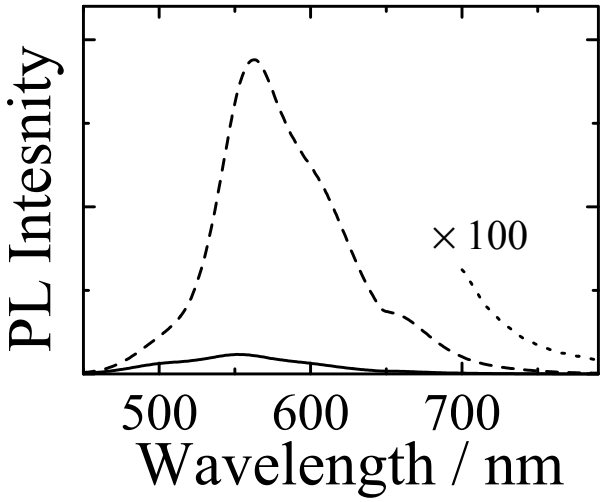

Figure 5. H. Ohkita et al.

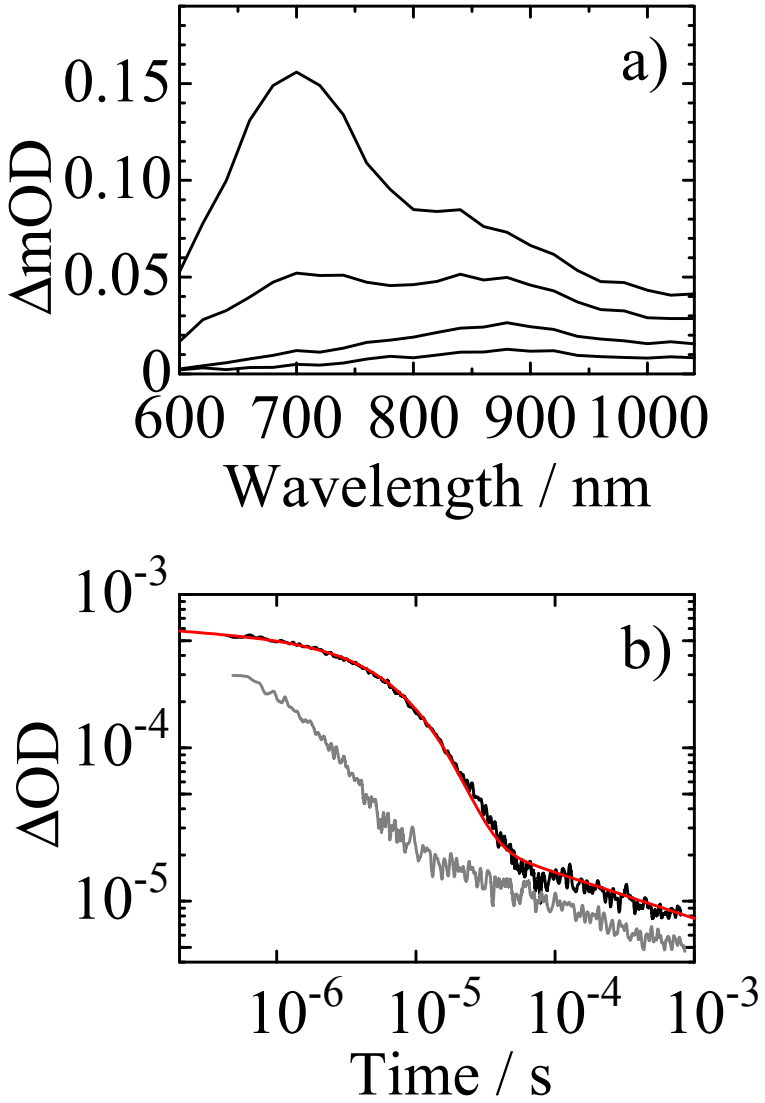

Figure 6. H. Ohkita et al.

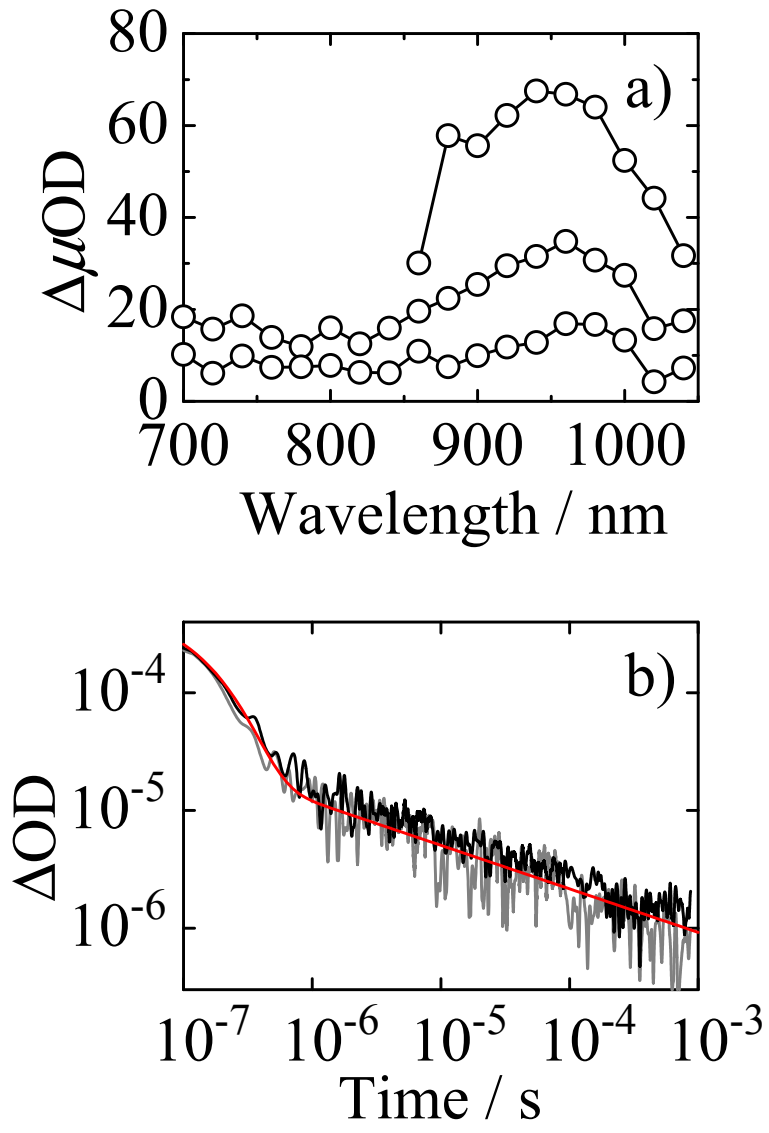

Figure 7. H. Ohkita et al.

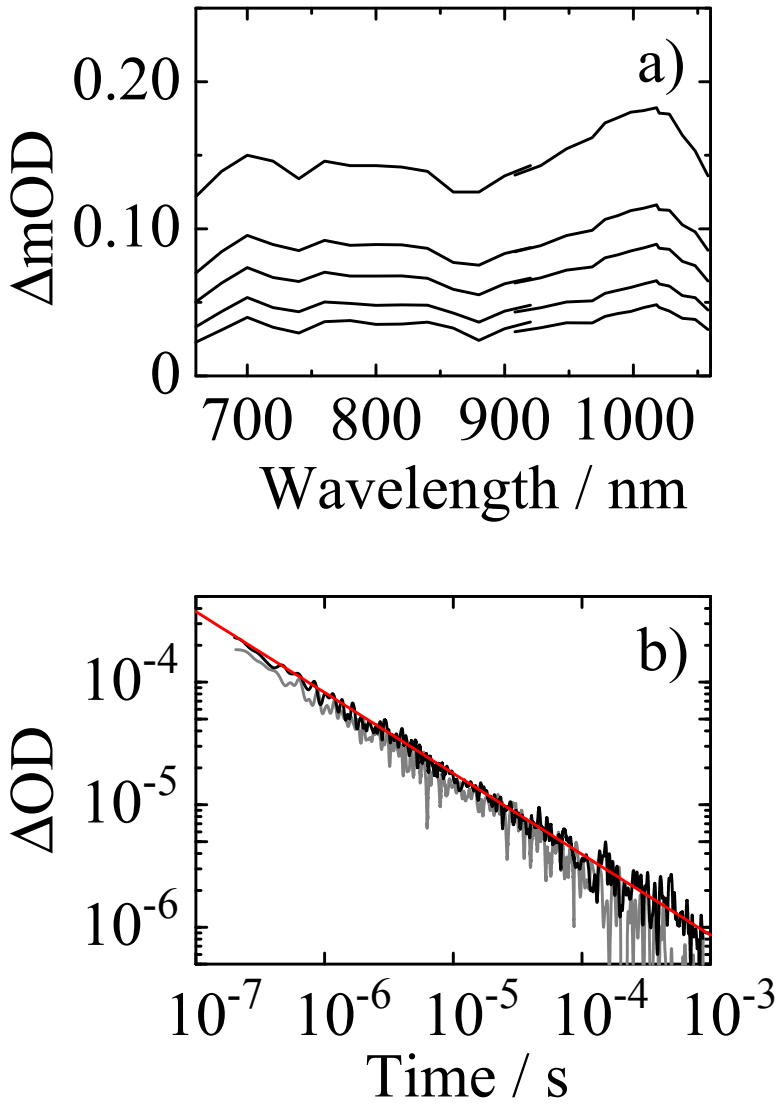

Figure 8. H. Ohkita et al.

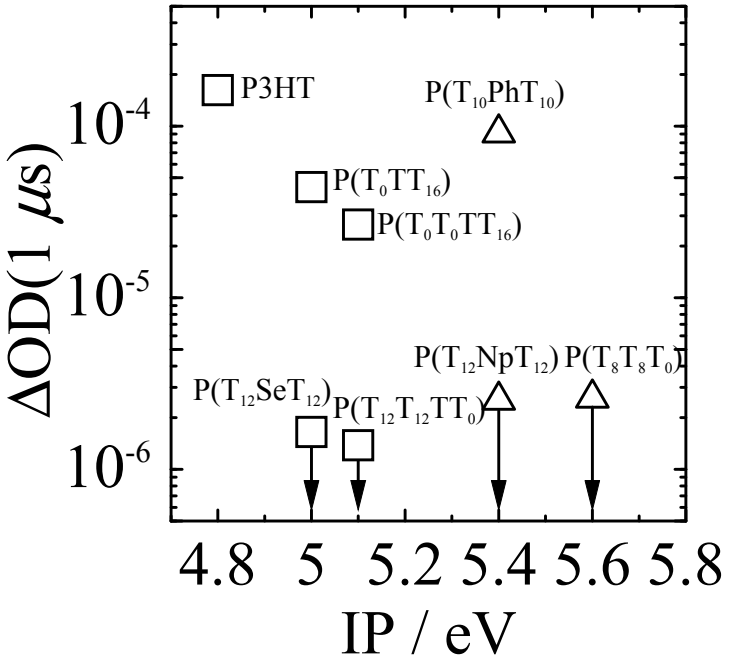

Figure 9. H. Ohkita et al.

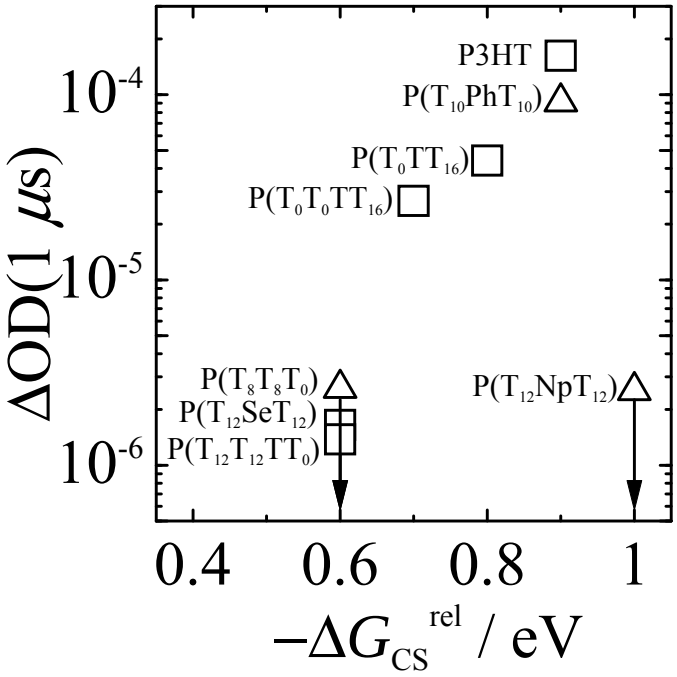

Figure 10. H. Ohkita et al.

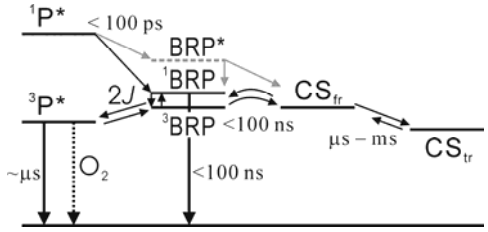

Scheme 1. H. Ohkita et al.

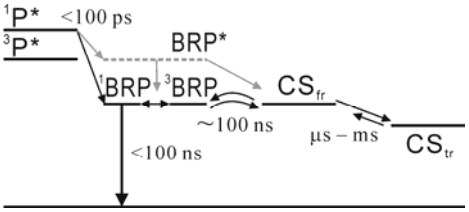

Scheme 2. H. Ohkita et al.

Table of Contents